Biophysical Chemistry 140 (2009) 99–107

Contents lists available at ScienceDirect

Biophysical Chemistry

journal homepage: http://www.elsevier.com/locate/biophyschem

Pressure-sensitive nutrient consumption via dynamic normal stress in rotational bioreactors

Laurence A. Belfiore [a,b,*], Walter Bonani [b], Matteo Leoni [b], Carol J. Belfiore [a]

[a] Department of Chemical & Biological Engineering, Colorado State University, Fort Collins, Colorado, 80523, USA
[b] Department of Materials Engineering & Industrial Technologies, University of Trento, via Mesiano 77, 38050 Trento, Italy

ARTICLE INFO

Article history:
Received 6 October 2008
Received in revised form 25 November 2008
Accepted 25 November 2008
Available online 7 December 2008

Keywords:
Rotational bioreactor
Nutrient consumption
Diffusion equation
Fick's second law
Pressure-sensitive reactions
Centrifugal force
Normal stress
Bone cell proliferation
Pressure-sensitive Damköhler number

ABSTRACT

Pressure-sensitive biological response is simulated in "rotating-cup" bioreactors with unidirectional modulations in compressive stress at the cylindrical wall that stimulate bone-tissue growth. Anchorage-dependent mammalian cells (i) adhere to a protein coating, (ii) receive nutrients and oxygen from an aqueous medium via radial diffusion toward the active surface, and (iii) respond to physiological modulations in centrifugal-force-induced fluid pressure at the cell/aqueous-medium interface. This process is modeled by the classic diffusion equation (i.e., Fick's second law), with a time-dependent reaction/diffusion boundary condition at the wall. Non-reversing angular velocity modulations resemble pulsations at physiological frequencies. Computer simulations of nutrient consumption profiles suggest that rotational bioreactor designs should consider the effects of normal stress when the pressure-sensitive Damköhler number (i.e., ratio of the pressure-dependent zeroth-order rate of nutrient consumption relative to the rate of nutrient diffusion toward active cells adhered to the cylindrical wall), evaluated under steady rotation, is greater than ≈10–20% of the stress-free Damköhler number (i.e., $\beta_{0,1st\text{-}order}=0.025$) for simple 1st-order stress-free kinetics, and ≈1% of the stress-free Damköhler number (i.e., $\beta_{0,2nd\text{-}order}=0.40$) for complex 2nd-order stress-free nutrient consumption. When the peak-to-peak amplitude of angular velocity modulations of the cylindrical wall is the same as or larger than the angular velocity for steady rotation, the effect of non-reversing centrifugal-force-induced dynamic normal stress in rotational bioreactors, superimposed on steady rotation, can be significant when one is below the critical value of the pressure-sensitive Damköhler number that has been identified under steady rotation.

1. Introduction

Rotational bioreactors can impose shear or compressive stress on anchorage-dependent cells to stimulate proliferation [1]. In this investigation, non-reversing dynamic normal stress at physiological frequencies is superimposed on "constant pressure at the cylindrical wall" to analyze effects on nutrient consumption. In the absence of continuous flow, nutrient depletion in the aqueous medium is described by the diffusion equation with a time-dependent reaction/diffusion boundary condition at the wall, enhanced by centrifugal-force-induced normal stress. Assistance from non-equilibrium thermodynamics provides a fundamental approach to describe stress-dependent nutrient consumption at the cell/aqueous-medium interface [2]. Under isotropic conditions where the transport coefficients are scalars, flux-i is coupled to force-j if the tensorial ranks of flux-i and force-j are the same or if they differ by an even integer [3–5]. This classic theorem for flux-force relations is known as the Curie restriction in isotropic systems, proposed by P. Curie in 1903 [3]. As a consequence of Curie's theorem in N-component systems, via the transport-phenomena-based rate of entropy production per volume of fluid, there are N first-rank tensorial fluxes that are coupled to N first-rank tensorial forces via linear laws [5]. Soret diffusion and Dufour conduction represent examples of these couplings between vector fluxes and driving forces in heat and mass transfer [6,7]. Curie's theorem predicts that scalar rates of production of the mass of species i due to chemical reaction should be coupled to the velocity gradient tensor, but this coupling is typically discarded based on physical rather than mathematical arguments [4], even though experiments have not been designed to investigate this unusual coupling [3]. If Curie's theorem is interpreted rigorously, then it becomes possible to describe quantitatively how normal pressure stress at the cell/aqueous-medium interface influences the scalar rate of nutrient consumption, because there is a connection between nutrient consumption and anchorage-dependent proliferation of bone cells, where the latter is stimulated by compressive stress [8,9]. There is experimental evidence in the research literature that low-amplitude high-frequency (i.e., 30 Hz) mechanical strain stimulates the proliferation of cancellous bone [10]. Hence, dynamic angular velocity modulations are included in this investigation, as well as Fourier analysis of these modulations via the fluctuation-dissipation theorem [4] to quantify the effect of frequency on

* Corresponding author. Presently at: Department of Materials Engineering & Industrial Technologies, University of Trento, via Mesiano 77, 38050 Trento, Italy.
E-mail address: belfiore@engr.colostate.edu (L.A. Belfiore).

0301-4622/$ – see front matter © 2008 Elsevier B.V. All rights reserved.
doi:10.1016/j.bpc.2008.11.015

entropy generation and nutrient consumption. The description and analysis of "rotating-cup" bioreactors are specific to the consumption of nutrients by anchorage-dependent bone cells bound to the protein-coated cylindrical wall. Non-equilibrium thermodynamics is employed to describe rates of nutrient consumption in biological systems that are stimulated by normal stress at the cell/aqueous-medium interface. Theoretical analysis and computer simulations in this research contribution are influenced strongly by the construction of linear transport laws in chemically reactive systems that obey Curie's theorem, which predicts the existence of cross-phenomena between fluxes (i.e., scalar reaction rates) and driving forces (i.e., second-rank velocity gradient tensor) whose tensorial ranks differ by an even integer—in this case, two. This example of scalar cross-phenomena is extrapolated to include effects of normal stress on nutrient consumption when centrifugal-force-induced contributions to fluid pressure are modulated by rotation of the cylindrical wall. There is experimental evidence that centrifugal force fields can be employed to seed cells in porous polymeric scaffolds [11]. The methodology described herein introduces a pressure-sensitive zeroth-order contribution to heterogeneous reaction rates that must be quenched via *Heaviside step functions* when nutrients or oxygen are not available for consumption. This bioreactor model is based on the unsteady state diffusion equation (i.e., Fick's second law) with a time-dependent reaction/diffusion boundary condition due to harmonic modulations in fluid pressure at the rotating cylindrical wall. There are essentially no publications in the research literature that match the following combination of keywords: *bioreactor*, *diffusion*, *centrifugal force*, *pressure-sensitive nutrient consumption*.

2. Development of the pressure-sensitive bioreactor model

2.1. Receptor-mediated cell-protein binding

Active poly(amino acid) sites are identified by favourable protein conformations within an aqueous layer on the inside surface of the cylindrical wall (i.e., at $r=R_{\text{wall}}$) that expose functional groups which participate in interactions with cell receptors. Stronger chemical bonds between adjacent receptors, due to the formation of receptor complexes, and stronger cell-protein binding energies increase cell fractional surface coverage. Larger exothermic binding energies (i.e., greater affinity) are consistent with an increase in the activation energy for desorption (i.e., same barrier energy but a deeper potential well in the adsorbed state), a decrease in the kinetic rate constant for desorption, an increase in the equilibrium constant for protein-ligand binding, and an increase in the equilibrium fraction of active protein sites that are occupied by cell receptors. Centrifugal force fields between 35 g and 52 g, via rotation at 2500 rpm, have been employed previously [11] to seed smooth muscle cells in porous poly(glycolic acid) scaffolds.

2.2. Stress-free rate of nutrient consumption

Within reasonable physiological limits, 2nd-order *stress-free* heterogeneous reaction rates for nutrient consumption are expressed in terms of (i) nutrient mass density on the inside surface of the cylindrical wall, $\rho_{\text{Nutrient}}(r=R_{\text{wall}},\boldsymbol{t})$, and (ii) oxygen mass density on the inside surface of the cylindrical wall, $\rho_{\text{Oxygen}}(r=R_{\text{wall}},\boldsymbol{t})$. Both mass densities have dimensions of mass per volume of the aqueous medium. Hence, the *stress-free* rate of nutrient consumption, with dimensions of nutrient mass per surface area per time, is;

$$-R_{A,SurfaceRx} = k_{2,Surface}\{\rho_{Nutrient}\}_{r=R_{wall}}\{\rho_{Oxygen}\}_{r=R_{wall}}. \tag{1}$$

Eq. (1) provides a mathematical representation of the rate of nutrient consumption at the cell/aqueous-medium interface, in which nutrients and dissolved oxygen are consumed by protein-bound bone cells such that nutrients and oxygen do not occupy protein sites on the active surface.

3. Stoichiometric requirement via diffusion in the aqueous boundary layer adjacent to the cylindrical wall

One invokes a balance between diffusion and reaction at the cylindrical wall in this rotational bioreactor. Nutrients diffuse radially outward toward anchorage-dependent cells, as specified by the rate of nutrient consumption. There exists a relation between nutrient and oxygen diffusional mass fluxes in the radial direction, evaluated at the wall, according to the cascade of physiological reactions that occur. The heterogeneous nature of this bioreactor design restricts the applicability of stoichiometry between nutrients and oxygen to the cylindrical wall at $r=R_{\text{wall}}$, where consumption occurs. Hence, at the well-defined cell/aqueous-medium boundary, the appropriate relation between diffusional mass fluxes, with dimensions of mass per area-time is;

$$\frac{1}{\varepsilon_{Nutrient}}D_{Nutrient}\left\{\frac{\partial\rho_{Nutrient}}{\partial r}\right\}_{r=R_{wall}} = \frac{1}{\varepsilon_{Oxygen}}D_{Oxygen}\left\{\frac{\partial\rho_{Oxygen}}{\partial r}\right\}_{r=R_{wall}}. \tag{2}$$

Since each side of Eq. (2) depends on time t, integration from initial time $t_{initial}$ to present time t yields the following approximation for the time-dependent mass density of oxygen near the cylindrical wall, which is required for quantitative evaluation of the rate of nutrient consumption;

$$\rho_{Oxygen}(r=R_{wall},t) = \rho_{Oxygen}(r=R_{wall},t=t_{initial}) - \frac{\varepsilon_{Oxygen}D_{Nutrient}}{\varepsilon_{Nutrient}D_{Oxygen}}\{\rho_{Nutrient}(r=R_{wall},t=t_{initial}) - \rho_{Nutrient}(r=R_{wall},t)\}. \tag{3}$$

Ordinary molecular diffusion coefficients for nutrients and oxygen in the aqueous medium scale inversely with the square-root of molecular weight [12], $\varepsilon_{\text{Oxygen}}/\varepsilon_{\text{Nutrient}}$ (i.e., ≈2–4%) represents the ratio of oxygen mass depleted relative to nutrient mass depleted during nutrient consumption, and within reasonable physiological limits, the initial mass density of dissolved oxygen is approximately 5–7% of the initial nutrient mass density. If the stoichiometry of oxygen-to-nutrient consumption is affected when bone cells are subjected to normal stress, then the initial condition in Eq. (3) should consider this modification to guarantee that a sufficient amount of oxygen is available for aerobic nutrient consumption.

4. Linear law for pressure-sensitive rates of nutrient consumption

If one focuses on fluxes and driving forces that appear as products in the rate of entropy generation per unit volume s_G for binary mixtures, from the transport-phenomena-based equation of change for fluid entropy [4];

$$s_G = \left\{\begin{array}{l} -\left(q_{Conduction} - \left[\frac{\mu_{A,ChemPotential}}{MW_A} - \frac{\mu_{B,ChemPotential}}{MW_B}\right]j_{A,Diffusion}\right)\bullet\frac{1}{T^2}\nabla T \\ -j_{A,Diffusion}\bullet\frac{1}{T}\left\{\left(g_{B,ForceField} - g_{A,ForceField}\right) + \nabla\left[\frac{\mu_{A,ChemPotential}}{MW_A} - \frac{\mu_{B,ChemPotential}}{MW_B}\right]\right\} \\ -R_{A,SurfaceRx}\frac{1}{T}\left[\frac{\mu_{A,ChemPotential}}{MW_A} - \frac{\mu_{B,ChemPotential}}{MW_B}\right] \\ -\tau_{ViscousStress} : \frac{1}{T}\{\nabla v\}_{VelocityGradientTensor} \end{array}\right\} \tag{4}$$

then Curie's theorem suggests that the scalar flux $-R_{\text{A,SurfaceRx}}$, better known as the rate of nutrient consumption, with dimensions of nutrient mass per surface area per time, should depend linearly on both scalar (i.e., $\mu_A/MW_A - \mu_B/MW_B$) and 2nd-rank tensor (i.e., ∇v) driving forces that appear on the right sides of the 3rd and 4th lines of s_G in Eq. (4). If necessary, $R_{\text{A,SurfaceRx}}$ can be written in pseudo-volumetric form via multiplication by the active-surface-to-volume ratio of the bioreactor, $=2/R_{\text{wall}}$. For pseudo-binary systems that are not far removed from *equilibrium*, the appropriate *linear law* for scalar cross-phenomena that satisfies Curie's restriction is written in the

following form for shear-stress-sensitive systems via the magnitude of the velocity gradient tensor [2]. Then, this coupling between zeroth-rank and 2nd-rank tensors is extrapolated to heterogeneous pressure-sensitive reactions when shear-free fluid motion produces centrifugal-force-induced normal stress at the wall;

Generalized kinetic rate law for stress–sensitive nutrient consumption

$$-R_{A,SurfaceRx} = \xi_{A1}\frac{1}{T}\left\{\frac{\mu_A}{MW_A}-\frac{\mu_B}{MW_B}\right\}+\xi_{A2}\frac{1}{T}\sqrt{\frac{1}{2}\{\nabla v\}:\{\nabla v\}^T}$$

Onsager coupling coefficients; ξ_{A1} *and* ξ_{A2}

$$\xi_{A1}=\alpha T;\ \xi_{A2}=\gamma T \tag{5}$$

Extrapolation to heterogeneous pressure–sensitive reactions

$$-R_{A,SurfaceRx} = k_{2,Surface}\{\rho_{Nutrient}\}_{r=R_{wall}}\left\{\rho_{Oxygen}\right\}_{r=R_{wall}} + \gamma\{p(r=R_{wall},\langle z\rangle,t)-p(r=0,z=0)-\rho g\langle z\rangle\}.$$

Linear approximations in the thermodynamics of irreversible processes that adequately describe transport phenomena under most experimental conditions are not very satisfactory for chemical reactions [4]. In general, large deviations from linear behaviour are observed for chemical reactions. Nonlinearity has been introduced in the reaction rate expression by focusing on the diagonal contribution due to *stress-free* chemical kinetics, not the contribution from normal pressure stress. Hence, the diagonal (i.e., scalar) contribution to the previous kinetic rate expression [i.e., Eq. (5)], based on differences between chemical potentials (i.e., *the affinity*), has been modified via Eq. (1) which corresponds to a second-order stress-free nonlinear rate law for biochemical reactions. The linear cross-term that accounts for pressure-sensitivity, relative to ambient and position-averaged hydrostatic pressure, should be appropriate at moderately low levels of centrifugal force that contribute to an increase in normal stress at the cylindrical wall. The form of Eq. (5) is sufficiently flexible to account for pressure effects at the active surface that might change the reaction pathway or the products of nutrient consumption if another parallel pathway were equally important, relative to the stress-free kinetic contribution. It should be emphasized that the linear laws of irreversible thermodynamics do not support the inclusion of pressure-dependence in the stress-free kinetic rate constant (i.e., ξ_{A1} or α) for nutrient consumption in pressure-sensitive systems. This is analogous to the fact that temperature-dependent diffusivities in Fick's first law (i.e., concentration diffusion) are not adequate to describe thermal diffusion, because an additional term that contains the gradient of temperature is required for coupled heat and mass transfer [6,7]. In contrast, transition state theory identifies the volume of activation, or the difference between partial molar volumes of the activated complex and all of the reactants, as the important factor that governs the pressure dependence of kinetic rate constants for gas phase reactions [13]. Volume changes that accompany the formation of the activated complex provide the dominant contribution to an exponential modification factor for kinetic rate constants at higher pressure [5,13]. The extrapolation to heterogeneous pressure-sensitive reactions in Eq. (5) does not follow the transition-state model which includes the volume of activation because pressure effects that might change the reaction pathway require an *additive* contribution to the rate law. Furthermore, the stoichiometry of nutrient consumption (i.e., mass of oxygen consumed per mass of nutrients consumed, $\varepsilon_{Oxygen}/\varepsilon_{Nutrient}$, and mass of cells generated per mass of nutrient consumed, $\varepsilon_{Cell}/\varepsilon_{Nutrient}$) might be different for stress-dependent rates of nutrient consumption relative to the stress-free consumption rates. Zeroth-order mechano-sensitive rates of nutrient consumption do not require stoichiometry to quantify the kinetic rate expression, but the initial condition should be modified to guarantee that a sufficient amount of oxygen is available for aerobic nutrient consumption.

5. Tangential fluid velocity for surface-driven flow with non-reversing angular velocity modulations

Unidirectional oscillatory motion of the cylindrical wall simulates steady and pulsatile normal stress on anchorage-dependent bone cells. The tangential fluid velocity component v_Θ scales linearly with radial position r via solid-body rotation at the interface between the nutrient medium and the cylindrical wall. The strategy to introduce physiological dynamic normal stress into this rotational bioreactor is accomplished by superposing modulated rotation and steady rotation [14]. Time-dependent *unidirectional* angular displacement $\Theta(t)$ and *non-reversing* angular velocity $d\Theta/dt$ of the cylindrical wall are expressed as follows and illustrated in Fig. 1;

$$\Theta(t) = \Omega t+\frac{1}{2}A\left\{t-\frac{\sin(\omega t)}{\omega}\right\}$$
$$\frac{d\Theta}{dt} = \Omega + A\sin^2\left(\frac{1}{2}\omega t\right). \tag{6}$$

Modulation frequency $\omega=2\pi\upsilon_{Heart}$ (i.e., $\upsilon_{Heart}\approx 1$ cycle/s) in Eq. (6) is the dominant frequency in the power spectrum when one considers the coupling between cardiac and respiratory oscillators in the regulation of blood flow, superimposed on random noise [15]. The volume of blood displaced per heartbeat is proportional to the peak-to-peak amplitude A ([=] rad/s) of dynamic angular velocity modulations [16], superimposed on steady rotation due to Ω. Time dependence of tangential fluid motion at the cylindrical wall mimics non-reversing harmonic modulations of the wall, according to the functional form of $d\Theta/dt$ in Eq. (6) and the *no-slip* condition, such that anchorage-dependent cells bound to active protein sites experience no shear stress, based on Newton's law [12]. If cells remain anchored to active protein sites, then there should be no conflict between the no-slip condition and elastic cell response in the presence of normal stress [17]. The enhancement in nutrient consumption due to the combined effects of steady and dynamic normal stress [18–20] is analogous to the increased sensitivity of calorimeter response during modulated differential scanning calorimetry experiments. The combination of steady and dynamic rotation of the cylindrical wall induces tangential fluid motion via Eq. (7);

$$v_\Theta(r,t) = f(r)\frac{d\Theta}{dt}. \tag{7}$$

Solid-body analysis of the rotating cylinder at $r=R_{wall}$ reveals that $f(r)=r$, which is consistent with the no-slip assumption and eliminates all components of viscous stress for Newtonian fluids [12], because the wall is in a *state of pure rotation*. The Θ-component of the Equation of

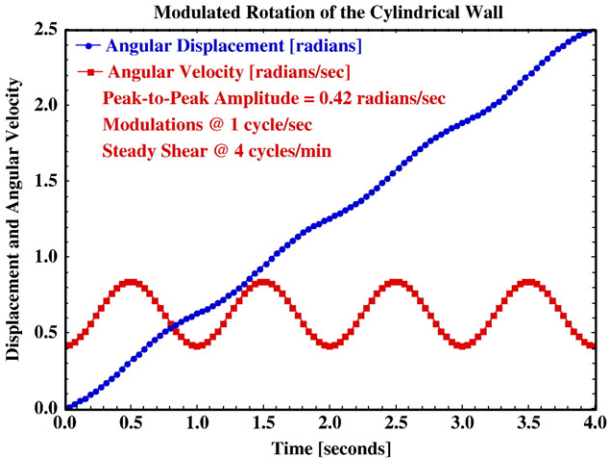

Fig. 1. Time-dependent angular displacement $\Theta(t)$ and angular velocity $d\Theta/dt$ of the cylindrical wall at $r=R_{wall}$, according to Eq. (6), simulating pulsatile normal stress in rotational bioreactors. Parametric values; $\Omega\approx 0.42$ rad/s (i.e., 4 rpm), $\omega=2\pi$ rad/s, peak-to-peak amplitude of angular velocity modulations $A=0.42$ rad/s.

Motion is satisfied in the creeping flow regime. Unless one seeks viscoelastic information associated with periodic motion of the wall, it is not necessary to describe modulations in angular displacement, angular velocity of the cylindrical wall, or the tangential linear fluid velocity component via exp{iωt}, with subsequent analysis of the real and imaginary responses. Hence, dynamic shear-free fluid motion with time-dependent pressure stress is described as follows;

$$v_\Theta(r,t) = r\left[\Omega + A\sin^2\left(\frac{1}{2}\omega t\right)\right]. \tag{8}$$

However, the viscous nature of the nutrient medium will introduce an oscillatory time lag that could be quantified via implementation of the "exp{iωt}-method" and consideration of $\rho\partial V_\partial/\partial t$ on the left side of the Θ-component of the Equation of Motion. The importance of $\rho\partial V_\partial/\partial t$ relative to viscous forces (i.e., oscillatory forces that produce an accumulation of momentum relative to force due to viscous momentum flux) scales as the product of the Reynolds and Strouhal numbers, which reduces to $\omega(R_{wall})^2/(\mu/\rho) \approx 18\pi/5$ for this "rotating-cup" bioreactor using the parameters described in the footnote to Table 1 (i.e., R_{wall} is the characteristic length). Steady and dynamic angular velocity of the wall should be restricted to ensure that the creeping flow requirement is satisfied at $r=R_{wall}$. Upon implementing a time-averaging procedure over one cycle of angular velocity modulations to estimate the tangential fluid velocity, the Reynolds number is constructed as follows;

$$\mathrm{Re} = \frac{\rho}{\mu}R_{wall}\left\{\frac{\omega}{2\pi}\int_0^{\frac{2\pi}{\omega}} v_\Theta(r=R_{wall},t)dt\right\} = \frac{\rho\omega R_{wall}^2}{2\pi\mu}\left\{\Theta\left(t=\frac{2\pi}{\omega}\right)-\Theta(t=0)\right\}$$
$$= \frac{\rho R_{wall}^2}{\mu}\left(\Omega+\frac{1}{2}A\right). \tag{9}$$

Table 1 summarizes the effect of the peak-to-peak amplitude of angular velocity modulations in v_Θ via Eq. (8) on the Reynolds number in Eq. (9). Hence, one predicts Reynolds numbers on the order of unity when the peak-to-peak amplitude of angular velocity modulations is the same as the magnitude of the angular velocity for steady rotation (i.e., 0.42 rad/s).

6. Normal pressure stress at the cylindrical wall

If the *z*-axis of the cylindrical configuration is vertical and independent variable z increases downward, such that $g_z=g$ and both g_r and g_Θ vanish, then the *r*- and Θ-components of the Equation of Motion reveal that fluid pressure depends on radial position *r*, due to centrifugal forces, and axial position *z*, due to gravity. It is difficult to impose a pressure gradient in the Θ-direction without the existence of normal viscous stress, like $\tau_{\theta\theta}$. One estimates modulations in fluid pressure at the cylindrical wall via "partial integration", as illustrated in Eq. (10), with assistance from Eq. (8);

$$\frac{\partial p}{\partial r} = \rho\frac{v_\Theta^2}{r} = \rho r\left[\Omega + A\sin^2\left(\frac{1}{2}\omega t\right)\right]^2$$
$$\frac{\partial p}{\partial z} = \rho g \tag{10}$$
$$p(r=R_{wall},z,t) = p(r=0,z=0) + \frac{1}{2}\rho R_{wall}^2\left[\Omega + A\sin^2\left(\frac{1}{2}\omega t\right)\right]^2 + \rho g z.$$

7. Diffusion equation for nutrient mass density

Bioreactor performance is established by calculating the mass density of nutrients from the diffusion equation (i.e., Fick's second law). Chemical reaction occurs only on the inside wall of the cylinder, which defines the interface between anchorage-dependent bone cells and the aqueous medium. Hence, nutrient consumption appears in the boundary conditions, but not in the mass balance [5]. The isothermal unsteady state diffusion equation is written in cylindrical coordinates;

$$\frac{\partial\rho_{Nutrient}}{\partial t} = D_{Nutrient}\frac{1}{r}\frac{\partial}{\partial r}\left\{r\frac{\partial\rho_{Nutrient}}{\partial r}\right\} \tag{11}$$

where $\rho_{Nutrient}$ corresponds to nutrient mass density, and $D_{Nutrient}$ is a concentration-independent molecular diffusion coefficient for nutrients in the aqueous culture medium. The axisymmetric nature of this bioreactor justifies the neglect of tangential convective mass transfer of nutrients, even though $v_\Theta \neq 0$ [21].

7.1. Zeroth-order pressure-sensitive rates of nutrient consumption at the cylindrical wall

A qualitative description of the boundary conditions considers a balance between the rate of nutrient transport toward the surface via molecular mass transfer and the rate of nutrient consumption that contains stress-free and pressure-sensitive contributions. The mathematical expression for this balance at $r=R_{wall}$ is;

$$-D_{Nutrient}\left\{\frac{\partial\rho_{Nutrient}}{\partial r}\right\}_{r=R_{wall}} = k_{2,Surface}\{\rho_{Nutrient}\}_{r=R_{wall}}\left\{\rho_{Oxygen}\right\}_{r=R_{wall}}$$
$$+\gamma H\{\rho_{Nutrient}(r=R_{wall},t)\}H\left\{\rho_{Oxygen}(r=R_{wall},t)\right\} \tag{12}$$
$$\{p(r=R_{wall},\langle z\rangle,t)-p(r=0,z=0)-\rho g\langle z\rangle\}.$$

Both processes have dimensions of nutrient mass per area of active protein sites per time, and the Onsager coupling coefficient γ has dimensions of inverse velocity. The pressure-sensitive contribution to the rate of nutrient consumption in Eq. (12) is classified as a zeroth-order reaction because it does not exhibit *explicit* dependence on the mass density of any species. However, this term must be extinguished when nutrients and oxygen (i.e., after a reasonable time lag when anaerobic proliferation is no longer feasible) are not available for immediate consumption by anchorage-dependent cells due to extreme diffusion-limited conditions in the aqueous medium. Zeroth-order rate laws must vanish in the absence of reactants [5]. This conceptual problem with the mathematical form of zeroth-order chemical reactions can be circumvented with assistance from *Heaviside step functions, $H\{\rho_{Nutrient}(r=R_{wall},t)\}$,* that terminate pressure-sensitive rates of nutrient consumption when reaction is sufficiently faster than radial diffusion at large Damköhler numbers. Computations that exclude step functions in the pressure-sensitive rate of nutrient consumption are vulnerable to the prediction of unrealistic negative species concentrations at the active boundary. Zero-flux, or symmetry, is invoked at $r=0$.

8. Dimensionless equations for unsteady-state radial diffusion with pressure-sensitive rates of nutrient consumption at the wall

8.1. Dimensionless variables and parameters

These design equations include radial diffusion and 2nd-order rates of nutrient consumption that depend on nutrient and oxygen mass density near the cylindrical wall. The problem description contains two important dimensionless parameters; (i) the ordinary Damköhler number, β_0, for stress-free heterogeneous chemical reactions (i.e., stress-free reaction rate divided by rate of radial diffusion), and (ii) the Damköhler number $\beta_{pressure}$ for pressure-sensitive heterogeneous chemical reactions at the cell/aqueous-

Table 1
Dependence of the Reynolds number on the peak-to-peak amplitude of angular velocity modulations of the cylindrical wall in rotational bioreactors

A [rad/s]	0	0.25	0.42	0.50	0.75	1.00
Reynolds #	0.76	0.98	1.13	1.21	1.43	1.66

Parameters; $R_{wall}=3$ mm, $\Omega=0.42$ rad/s, $\omega_{Heart}=2\pi$ rad/s.
$\mu/\rho=5\times10^{-2}$ cm^2/s.

medium boundary (i.e., normal-stress-dependent rate of reaction divided by the rate of nutrient diffusion toward anchorage-dependent cells). The angular velocity Ω of the cylindrical wall is a convenient experimental variable that allows one to perform systematic parametric sensitivity simulations based on the pressure-sensitive Damköhler number. If the *characteristic length* is R_{wall}, then;

$$\begin{aligned}
&\textit{Temporal independent variable; } t = \frac{\tau R_{wall}^2}{D_{Nutrient}}\\
&\textit{Radial independent variable; } r = \eta R_{wall}\\
&\textit{Nutrient mass density; } \rho_{Nutrient} = \rho_{Nutrient,Bulk}(t=0)\,\Psi_{Nutrient}\\
&\textit{Oxygen mass density; } \rho_{Oxygen} = \rho_{Nutrient,Bulk}(t=0)\,\Psi_{Oxygen}\\
&\textit{Stress-free Damkohler number } (n^{th}\textit{-order}); \beta_{0,} = \frac{R_{wall}k_{n,Surface}\rho_{Nutrient,Bulk}^{n-1}(t=0)}{D_{Nutrient}}\\
&\text{Pressure-}\textit{sensitive Damkohler number};\\
&\beta_{pressure} = \frac{\gamma R_{wall}\{p(r=R_{wall},\langle z\rangle;A=0)-p(r=0,z=0)-\rho g\langle z\rangle\}}{D_{Nutrient}\rho_{Nutrient,Bulk}(t=0)}\\
&\qquad = \frac{\gamma\rho\Omega^2R_{wall}^3}{2D_{Nutrient}\rho_{Nutrient,Bulk}(t=0)}.
\end{aligned} \tag{13}$$

The pressure-sensitive Damköhler number is constructed in terms of the centrifugal force contribution to fluid pressure at the cylindrical wall, with no modulations [i.e., $A=0$ in Eq. (10)].

8.2. Dimensionless diffusion equation

Nutrient mass density must satisfy the following partial differential equation via Fick's second law in cylindrical coordinates;

$$\frac{\partial\Psi_{Nutrient}}{\partial\tau} = \frac{1}{\eta}\frac{\partial}{\partial\eta}\left\{\eta\frac{\partial\Psi_{Nutrient}}{\partial\eta}\right\}. \tag{14}$$

The temporal derivative (i.e., with respect to t, or τ) is written using first-order-correct finite differences, whereas radial diffusion toward the aqueous protein coating on the cylindrical wall [i.e., 2nd-derivative with respect to r, or η, on the right side of Eq. (14)] is implicit at the new time step using second-order-correct finite-difference analogs.

8.3. Separability of the diffusion equation

It is possible to identify the nature of the radial and temporal functions [i.e., $F(\eta)$ and $G(\tau)$, respectively] that represent a separation-of-variables solution to Eq. (14), prior to generating numerical results. If $\Psi_{Nutrient}(\eta,\tau)=F(\eta)G(\tau)$, then the dimensionless diffusion equation reveals that;

$$\begin{aligned}
&\frac{d\ln G}{d\tau} = -\chi^2 \Rightarrow G(\tau)\approx\exp\{-\chi^2\tau\}\\
&\frac{d}{d\eta}\left\{\eta\frac{dF}{d\eta}\right\} + \chi^2\eta F(\eta) = 0
\end{aligned} \tag{15}$$

where χ is real such that $-\chi^2$ is a negative *separation constant* which prevents $G(\tau)$ from increasing unrealistically in unbounded fashion at large time. $F(\eta)$ is given by zeroth-order Bessel functions of the 1st kind [i.e., $J_0(\chi\eta)$].

8.4. Dynamic bioreactor analysis via the periodic boundary condition at the wall

Modulations of the cylindrical wall that simulate dynamic normal stress introduce time dependence into the reaction/diffusion boundary condition at $r=R_{wall}$. The dimensionless boundary condition which represents a balance between nutrient diffusion in the radial direction, toward the wall, and nutrient consumption contains both types of Damköhler numbers. All of the required boundary conditions are summarized below;

$$\begin{aligned}
&\Psi_{Nutrient} = 1 @ \tau = 0, 0 \le \eta < 1\\
&\left\{\frac{\partial\Psi_{Nutrient}}{\partial\eta}\right\}_{\eta=0} = 0\\
&-\left\{\frac{\partial\Psi_{Nutrient}}{\partial\eta}\right\}_{\eta=1} = \beta_0\Psi_{Nutrient}(\eta=1,\tau)\Psi_{Oxygen}(\eta=1,\tau) + H\{\Psi_{Nutrient}(\eta=1,\tau)\}\\
&\qquad H\{\Psi_{Oxygen}(\eta=1,\tau)\}\beta_{pressure}\Gamma(\eta=1,t;\omega)\\
&\Gamma(\eta,t;\omega) = \frac{p(r,\langle z\rangle,t)-p(r=0,z=0)-\rho g\langle z\rangle}{p(r=R_{wall},\langle z\rangle;A=0)-p(r=0,z=0)-\rho g\langle z\rangle} = \eta^2\left\{1+\frac{A}{\Omega}\sin^2\left(\frac{1}{2}\omega t\right)\right\}^2.
\end{aligned} \tag{16}$$

9. Evaluation of bioreactor performance

The most effective bioreactor design depletes nutrients and proliferates cells most rapidly under physiological conditions, yielding the smallest volume-averaged bulk nutrient mass density at time t, which is defined as follows;

$$\rho_{Nutrient,Bulk}(t) = \frac{2\pi L\int_{r=0}^{R_{wall}}\rho_{Nutrient}(r,t)rdr}{\pi R_{wall}^2 L} = 2\int_{\eta=0}^{\eta=1}\rho_{Nutrient}(\eta,t)\eta d\eta. \tag{17}$$

If the separation-of-variables solution for $\Psi_{Nutrient}(\eta,\tau)$, given by Eq. (15), is valid, then bulk nutrient mass density defined by Eq. (17) scales as $\exp(-\chi^2\tau)$.

$$\rho_{Nutrient,Bulk}(t)\approx\rho_{Nutrient,Bulk}(t=0)\exp\{-\chi^2\tau\}\int_{\eta=0}^{\eta=1}J_0(\chi\eta)\eta d\eta. \tag{18}$$

10. Computer simulations

10.1. Effect of steady rotation (i.e., Ω in $\beta_{pressure}$) on nutrient consumption for simple 1st-order and complex 2nd-order stress-free kinetics

Bulk nutrient mass density profiles in the presence of steady rotation (i.e., $A=0$) and constant normal stress at the cylindrical wall are illustrated in Fig. 2 vs. dimensionless time for 1st-order irreversible stress-free kinetics. The rate of nutrient consumption depends linearly

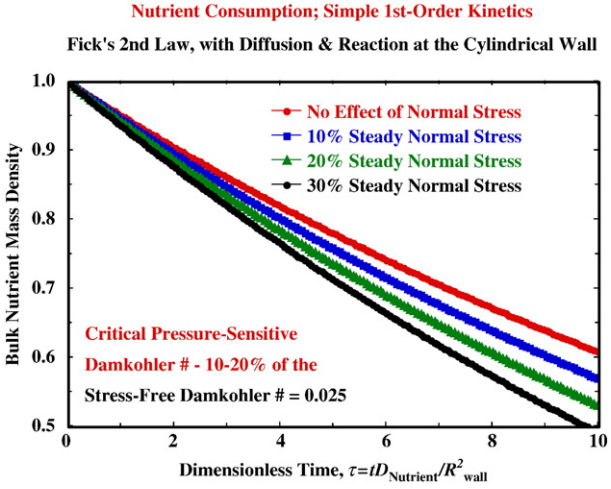

Fig. 2. Dimensionless bulk nutrient mass density profiles in rotational bioreactors at various pressure-sensitive Damköhler numbers when stress-free nutrient consumption follows 1st-order irreversible kinetics that depend only on nutrient mass density at the cylindrical wall. The legend should be interpreted as the ratio of the pressure-sensitive Damköhler number to the stress-free Damköhler number. This ratio increases from the uppermost curve to the lowermost curve, with no angular velocity modulations (i.e., A=0). The critical value of the pressure-sensitive Damköhler number is between 10% and 20% of the stress-free Damköhler number. Parameters: dimensionless step size in the r-direction, $\Delta\eta=0.010$; dimensionless step size in time, $\Delta\tau=6.4\times10^{-2}$.

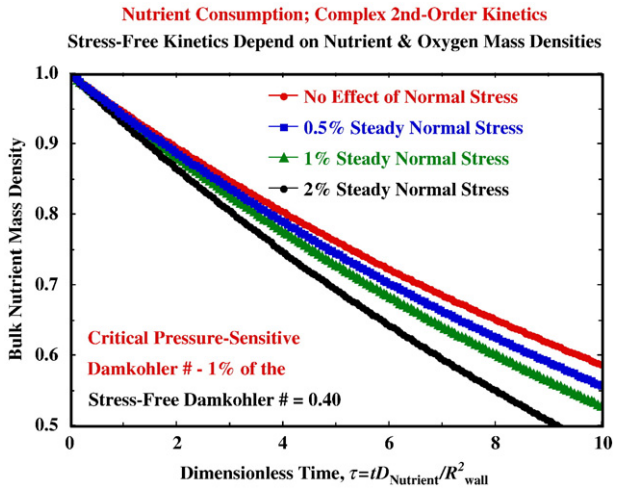

Fig. 3. Dimensionless bulk nutrient mass density profiles in rotational bioreactors at various pressure-sensitive Damköhler numbers when stress-free nutrient consumption follows complex 2nd-order irreversible kinetics described by Eq. (1). The legend should be interpreted as the ratio of the pressure-sensitive Damköhler number to the stress-free Damköhler number. This ratio increases from the uppermost curve to the lowermost curve, with no angular velocity modulations (i.e., A=0). The critical value of the pressure-sensitive Damköhler number is approximately 1% of the stress-free Damköhler number. Parameters: dimensionless step size in the r-direction, $\Delta\eta=0.010$; dimensionless step size in time, $\Delta\tau=6.4\times10^{-2}$. Nutrient molecular weight=1000 daltons; diffusivity ratio, $\delta_{Diffusivity}\approx\{32/1000\}0.5$; initial mass ratio of oxygen consumed to mass of nutrients, $\rho_{Oxygen}(t=0)/\rho_{Nutrient}(t=0)=0.07$ (i.e., 7%); ratio of mass of oxygen consumed to mass of nutrients consumed by cells adhered on protein-coated surface at the cylindrical wall, $\varepsilon_{Oxygen}/\varepsilon_{Nutrient}=0.04$ (i.e., 4%).

on nutrient mass density at the cylindrical wall. The stress-free Damköhler number (i.e., $\beta_{0,1st\text{-}order}$) is 0.025, indicative of a diffusion time constant (i.e., $R^2_{wall}/D_{Nutrient}$) that is 40-fold shorter than the time constant for chemical reaction (i.e., $R_{wall}/k_{1,Surface}$). Hence, these simulations in Fig. 2 do not represent the diffusion-controlled regime because the active surface at the cylindrical wall is not starved of nutrients or oxygen. The shape of these bulk nutrient mass density profiles is consistent with Eq. (18). The critical pressure-sensitive Damköhler number (i.e., $\beta_{pressure,critical}$) is between 10% and 20% of the stress-free Damköhler number. Hence, $\beta_{pressure,critical}\approx3\text{–}5\times10^{-3}$ when $\beta_{0,1st\text{-}order}$ is 0.025. When $\beta_{pressure}$ is larger than its critical value, one should include stress-sensitive zeroth-order nutrient consumption in the boundary condition at the cylindrical wall.

For complex second-order stress-free nutrient consumption described by Eq. (1), the effects of steady rotation and constant normal stress are illustrated in Fig. 3 vs. dimensionless time. The stress-free Damköhler number (i.e., $\beta_{0,2nd\text{-}order}$) has been increased 16-fold from 0.025 in Fig. 2 to 0.40 in Fig. 3 to achieve essentially the same stress-free nutrient consumption (≈40%) in Figs. 2 and 3 for a dimensionless observation time of 10. This combination of $\beta_{0,2nd\text{-}order}=0.40$ and $\tau=10$ corresponds to observation times t on the far right side of Fig. 3 that are 4-fold larger than the time constant for chemical reaction. Once again, bulk nutrient mass density profiles in Fig. 3 are not indicative of the diffusion-controlled regime, because the stress-free Damköhler number of 0.40 indicates that the diffusion time constant (i.e., $R^2_{wall}/D_{Nutrient}$) is 2.5-fold shorter than the time constant for 2nd-order chemical reaction [i.e., $R_{wall}/\{k_{2,Surface}\rho_{Nutrient,Bulk}(t=0)\}$]. Simulations in Fig. 3 reveal that the critical pressure-sensitive Damköhler number $\beta_{pressure,critical}$, above which stress-sensitivity in the reaction/diffusion boundary condition at the cylindrical wall must be considered, is approximately 1% of the stress-free Damköhler number. Hence, $\beta_{pressure,critical}\approx4\times10^{-3}$ when $\beta_{0,2nd\text{-}order}=0.40$, indicating that the critical pressure-sensitive Damköhler number for zeroth-order stress-sensitive reactions is not affected much by the kinetic model for stress-free nutrient consumption, because 10–20% of $\beta_{0,1st\text{-}order}$ in Fig. 2 is essentially the same as 1% of $\beta_{0,2nd\text{-}order}$ in Fig. 3.

11. Effect of the amplitude of angular velocity modulations [via A in $\Gamma(\eta,t;\omega)$] on nutrient consumption for complex stress-free kinetics

These simulations include time dependence in the reaction/diffusion boundary condition at the rotating cylindrical wall, due to angular velocity modulations and the effect of centrifugal force on fluid pressure. The primary objective is to demonstrate that stress-sensitive nutrient consumption must be included in this boundary condition when modulated rotation is superimposed on steady rotation, and the pressure-sensitive Damköhler number is below its critical value that has been determined from steady rotation simulations in Fig. 3. Bioreactor performance at sub-critical Damköhler numbers in Fig. 4 when $A=\Omega=4$ revolutions/min. is distinguishable from the stress-free nutrient consumption profile because centrifugal-force-induced pressure-sensitive response scales as the square of angular velocity modulations. Bulk nutrient mass density oscillations at 1 Hz are observed in the lower curve of Fig. 4 when the peak-to-peak amplitude of angular velocity modulations (i.e., A) matches the magnitude of steady rotation Ω, but no other effects of frequency on the rate of nutrient consumption are predicted. This deficiency in the pressure-sensitive dynamic model is addressed in the next section.

12. Auto-correlation of normal stress modulations via the fluctuation-dissipation theorem identifies frequency-dependent nutrient consumption rates

Another approach to describe the effect of modulation frequency on nutrient consumption is discussed from the viewpoint of energy dissipation and entropy generation. According to Callen and Welton [22], systems exhibit *dissipative* characteristics if they are capable of absorbing energy in response to perturbations that fluctuate periodically in time. For systems under the influence of time-dependent excitations, the fluctuation-dissipation theorem relates correlation functions for periodic disturbances to dissipation processes that generate entropy [4]. If the dimensionless time-dependent ratio of fluid pressure, with and without angular velocity modulations,

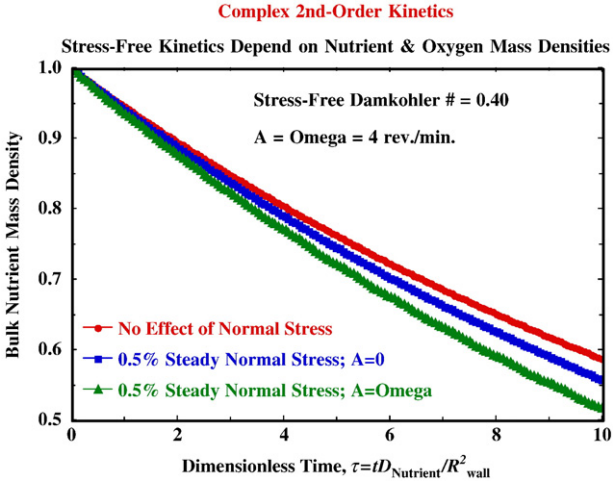

Fig. 4. Dimensionless bulk nutrient mass density profiles in rotational bioreactors when stress-free nutrient consumption follows complex 2nd-order irreversible kinetics described by Eq. (1) and the pressure-sensitive Damköhler number is below its critical value, determined via simulations in Fig. 3. The effect of dynamic normal stress, superimposed on steady rotation at 0.42 rad/s, is operative when the peak-to-peak amplitude of angular velocity modulations at 1 Hz matches the magnitude of steady rotation (i.e., $A=\Omega$ in the lowest curve). Parameters: dimensionless step size in the r-direction, $\Delta\eta=0.010$; dimensionless step size in time, $\Delta\tau=6.4\times10^{-2}$; nutrient molecular weight=1000 Da; diffusivity ratio, $\delta_{Diffusivity}\approx\{32/1000\}^{0.5}$; initial mass ratio of oxygen to nutrients, $\rho_{Oxygen}(t=0)/\rho_{Nutrient}(t=0)=0.07$ (i.e., 7%); ratio of mass of oxygen consumed to mass of nutrients consumed by cells adhered on protein-coated surface at the cylindrical wall, $\varepsilon_{Oxygen}/\varepsilon_{Nutrient}=0.04$ (i.e., 4%).

experienced by anchorage-dependent cells at the cylindrical wall [i.e., $\Gamma(\eta,t;\omega)$ in Eq. (16)] is auto-correlated via time-averaging over one cycle of oscillation, then;

$$\sigma(\eta=1,\omega,\tau)=\langle\Gamma(\eta=1,t;\omega)\Gamma(\eta=1,t+\tau;\omega)\rangle_{time\text{-}averaged} \quad (19)$$
$$=\frac{\omega}{2\pi}\int_0^{\frac{2\pi}{\omega}}\Gamma(\eta=1,t;\omega)\Gamma(\eta=1,t+\tau;\omega)dt.$$

In Eqs. (19)–(22), τ is a dimensional time variable used to auto-correlate and Fourier transform dynamic normal stress at the cylindrical wall via angular velocity modulations. One-sided Fourier transformation of $\sigma(\eta=1,\omega,\tau)$ yields a complex power spectrum $S(\omega)$ via the Wiener-Khinchin-Einstein theorem [4]. Hence;

$$S(\omega)=\int_{\tau=0}^{\tau\Rightarrow\infty}\sigma(\eta=1,\omega,\tau)\exp(-i\omega\tau)d\tau \quad (20)$$
$$=\int_{\tau=0}^{\tau\Rightarrow\infty}\sigma(\eta=1,\omega,\tau)\cos(\omega\tau)d\tau-i\int_{\tau=0}^{\tau\Rightarrow\infty}\sigma(\eta=1,\omega,\tau)\sin(\omega\tau)d\tau.$$

The fluctuation-dissipation theorem allows one to express the real and imaginary parts of $S(\omega)$ in terms of the imaginary and real parts, respectively, of a complex susceptibility $\kappa(\omega)$;

$$\kappa(\omega)=i\omega S(\omega)=\omega\int_{\tau=0}^{\tau\Rightarrow\infty}\sigma(\eta=1,\omega,\tau)\sin(\omega\tau)d\tau \quad (21)$$
$$+i\omega\int_{\tau=0}^{\tau\Rightarrow\infty}\sigma(\eta=1,\omega,\tau)\cos(\omega\tau)d\tau.$$

The real and imaginary parts of $\kappa(\omega)$ are related by the Kramers-Kronig theorem [4,23,24]. The imaginary part of $\kappa(\omega)$ represents the *frequency-dependent absorption* or *energy dissipation function* [25] for pulsatile normal stress experienced by anchorage-dependent cells attached to the cylindrical wall. Hence, the cosine transform of the auto-correlation function for angular velocity modulations, via centrifugal force contributions to fluid pressure, maps out the characteristic frequencies of periodic disturbances associated with entropy generation. The fluctuation-dissipation theorem in non-equilibrium thermodynamics provides an alternate route to quantify the effect of dynamic normal stress on enhanced rates of nutrient consumption, in response to pulsatory disturbances at higher frequency. The reaction/diffusion boundary condition at the cylindrical wall is written as follows;

$$-D_{Nutrient}\left\{\frac{\partial\rho_{Nutrient}}{\partial r}\right\}_{r=R_{wall}}=k_{2,Surface}\{\rho_{Nutrient}\}_{r=R_{wall}}\left\{\rho_{Oxygen}\right\}_{r=R_{wall}}$$
$$+\gamma' H\{\rho_{Nutrient}(r=R_{wall},t)\}H\left\{\rho_{Oxygen}(r=R_{wall},t)\right\}$$
$$\omega\int_{\tau=0}^{\tau\Rightarrow\infty}\sigma(\eta=1,\omega,\tau)\cos(\omega\tau)d\tau. \quad (22)$$

where the modified Onsager coefficient γ' has dimensions of mass per area of active protein sites per time. The essence of the *fluctuation-dissipation theorem* in statistical physics [4,26] focuses on periodic involuntary fluctuations in cardiovascular flow that can be *auto-correlated* and Fourier transformed to reveal how these disturbances contribute to pressure-sensitive rates of nutrient consumption at the cylindrical wall. Hence, frequency dependence of periodic cardiovascular stress can be included in the reaction/diffusion boundary condition.

13. Self-consistent check of the microscopic solutions via the unsteady state macroscopic mass balance

It is not unreasonable to suspect that truncation errors in the numerical approximation of 1st- and 2nd-derivatives might accumulate in the computational scheme used to integrate the diffusion equation, together with diffusion and reaction at the cylindrical wall. In the absence of exact analytical solutions, the following internal self-consistent approach was employed to verify accuracy of the microscopic results. One integrates the diffusion equation [i.e., Eq. (11) or (14)] over the macroscopic volume of this rotational bioreactor (i.e., $\pi R^2_{wall}L$). The volume integral of the divergence of diffusional flux is converted to surface integrals via Gauss' law. Then, diffusional mass flux of nutrients evaluated at the cylindrical wall is replaced by the rate of nutrient consumption via the diffusion/reaction boundary condition [i.e., Eq. (12) or (16)] to obtain the following unsteady state macroscopic balance for bulk nutrient mass density;

$$-\pi R^2_{wall}L\frac{d\rho_{Nutrient,Bulk}}{dt}=2\pi R_{wall}L\left\{\begin{array}{l}k_{2,Surface}\{\rho_{Nutrient}\}_{r=R_{wall}}\left\{\rho_{Oxygen}\right\}_{r=R_{wall}}+\\ \gamma H\{\rho_{Nutrient}(r=R_{wall},t)\}H\left\{\rho_{Oxygen}(r=R_{wall},t)\right\}[p(r=R_{wall},\langle z\rangle,t)-p(r=0,z=0)-\rho g\langle z\rangle]\end{array}\right\}. \quad (23)$$

The dimensionless version of Eq. (23) is;

$$\frac{d\Psi_{Nutrient,Bulk}}{d\tau}=-2\left\{\begin{array}{l}\beta_0\{\Psi_{Nutrient}\}_{\eta=1}\{\Psi_{Oxygen}\}_{\eta=1}+\\ \beta_{pressure}H\{\Psi_{Nutrient}(\eta=1,\tau)\}H\{\Psi_{Oxygen}(\eta=1,\tau)\}\Gamma(\eta=1,\tau;\omega)\end{array}\right\}. \quad (24)$$

Finite-difference solutions of the diffusion equation with diffusion and reaction at the cylindrical wall yield a discrete local nutrient mass density profile, $\rho_{Nutrient}(r,\boldsymbol{t})$, that is (i) evaluated at $r=R_{wall}$ (i.e., $\eta=1$) to predict rates of nutrient consumption by anchorage-dependent cells bound to a protein-coating, and (ii) integrated over the total volume of the system to generate bulk nutrient mass density, $\rho_{Nutrient,Bulk}(\boldsymbol{t})$ via Eq. (17). Then, $\rho_{Nutrient,Bulk}$ is differentiated numerically with respect to time to obtain the quantity on the left side of Eq. (23). All finite-difference results generated in this investigation exhibit internal self-consistency and satisfy the unsteady state macroscopic mass balance to within 3×10^{-4} %, via the ratio of the left-side to the right-side of Eq. (24).

14. Unusual characteristics of this bioreactor analysis

There are a few aspects of this investigation that deviate significantly from the traditional design of ordinary batch chemical reactors. (1) Kinetic rate expressions that describe nutrient consumption are modified for normal-stress-sensitive reactions, based on an extension of the formalism of scalar cross-phenomena in the thermodynamics of irreversible processes. (2) Pressure-sensitive zeroth-order contributions to the rate of nutrient consumption are quenched via Heaviside step functions when cells are starved of either nutrients or oxygen due to extreme diffusion-controlled conditions within the diffusion boundary layer adjacent to the aqueous protein coating on the cylindrical wall. (3) Flexibility in the rate of nutrient consumption for pressure-sensitive biological systems is included to

account for centrifugal-force-induced increases in normal stress at the active surface that might affect the reaction pathway, the stoichiometry of nutrient consumption, and/or the products of nutrient consumption if another parallel pathway is equally important. (4) The complete problem description is developed in terms of mass density, not molar density, because cell physiology and the cascade of events that describe nutrient consumption are treated phenomenologically via analogous processes in heterogeneous catalysis.

15. Conclusions

There have not been many predictive simulations that focus on the interplay between diffusion and reaction in biological systems, when nutrient consumption by anchorage-dependent cells exhibits stress-sensitivity. In this research contribution, the effect of centrifugal-force-induced steady and dynamic normal stress on rates of nutrient consumption by bone cells adhered to active protein sites on the inside wall of a "rotating-cup" bioreactor has led to the identification of the critical pressure-sensitive Damköhler number. Above this critical ratio of the normal-stress-sensitive zeroth-order rate of nutrient consumption relative to the rate of nutrient diffusion toward anchorage-dependent mammalian cells at the boundary of the rotating-cylinder configuration, one must include contributions from compressive stress in the reaction/ diffusion boundary condition to obtain accurate predictions of reactor performance.

Curie's law in non-equilibrium thermodynamics states that rates of chemical reaction are coupled, in principle, to some scalar representation of the velocity gradient tensor [2–5]. This coupling has been extended to describe the effect of centrifugal-force-induced dynamic normal stress on nutrient consumption in rotational bioreactors when compressive stress stimulates cell proliferation. Based on formalism in the thermodynamics of irreversible processes, one adds a stress-sensitive rate of consumption to standard stress-free rates, where the latter contain nonlinear effects via the analogy with heterogeneous catalysis. Theoretical analysis and computer simulations of nutrient mass density in "rotating-cup" bioreactors, based on Fick's second law of diffusion with a time-dependent reaction/diffusion boundary condition at the cylindrical wall, allow one to identify conditions when stress-sensitive nutrient consumption cannot be neglected. Complex 2nd-order stress-free kinetics require the presence of nutrients and oxygen at the cylindrical wall, for consumption to spawn proliferation. Under these conditions, stress-sensitive ratios of consumption rate to diffusion rate should be greater than 1% of the analogous stress-free ratio before bioreactor designs must consider mechano-sensitive zeroth-order contributions to the overall rate of nutrient consumption. The absolute magnitude of the critical pressure-sensitive Damköhler number $\beta_{\text{pressure,critical}}$ for zeroth-order stress-sensitive reactions is not affected much by the kinetic model for stress-free rates of nutrient consumption. When angular velocity modulations of the cylindrical wall are introduced to mimic physiological pulsations, simulations reveal that pressure-sensitive rates of nutrient consumption could be important when rotational bioreactors operate below $\beta_{\text{pressure,critical}}$, which has been identified under steady rotation. Rates of entropy generation from the viewpoint of the fluctuation-dissipation theorem and non-equilibrium thermodynamics are invoked to provide a better description of the effect of pulsation frequency on pressure-sensitive rates of nutrient consumption in the reaction/diffusion boundary condition at the rotating cylindrical wall.

Nomenclature

A peak-to-peak amplitude of angular velocity modulations of the cylindrical wall at $r=R_{\text{wall}}$ (i.e., $A \leq 0.42$ rad/s)

D_{Nutrient} ordinary molecular diffusion coefficient of nutrients in aqueous mixtures; length^2 per time

D_{Oxygen} ordinary molecular diffusion coefficient of dissolved oxygen in aqueous mixtures; length^2 per time

$F(\eta)$ radial contribution to the separation-of-variables solution for dimensionless nutrient mass density, $\Psi_{\text{Nutrient}}(\eta,\tau)$

$g_{i,\text{ForceField}}$ force per unit mass exerted on species i due to the gravitational field

$G(\tau)$ temporal contribution to the separation-of-variables solution for dimensionless nutrient mass density, $\Psi_{\text{Nutrient}}(\eta,\tau)$

$H(x)$ Heaviside step function

$J_0(\chi\eta)$ zeroth-order Bessel function of the 1st-kind; radial contribution to the separation-of-variables solution for nutrient mass density

$j_{\text{A,Diffusion}}$ diffusional mass flux of species A; dimensions of species mass per area-time

$k_{1,\text{Surface}}$ kinetic rate constant for 1st-order stress-free nutrient consumption; length/time

$k_{\text{n,Surface}}$ kinetic rate constant for stress-free heterogeneous rate of nutrient consumption via nth-order reaction (i.e., n=2) that depends on nutrient and oxygen mass density at the cylindrical wall; $\{\text{volume/mass}\}^{n-1}\bullet$length/time

L length of the cylindrical bioreactor

MW_i molecular weight of species i

$q_{\text{Conduction}}$ molecular flux of thermal energy; dimensions of energy per area-time

r independent radial variable that increases as one moves toward the wall of the "rotating-cup" bioreactor

Δr step size in the radial direction, between grid points

$-R_{\text{A,SurfaceRx}}$ stress-free heterogeneous rate of nutrient consumption; mass per area-time

R_{wall} radius of the cylindrical bioreactor

s_G rate of entropy generation in binary mixtures; dimensions of entropy per volume-time

S frequency-dependent spectral density or power spectrum obtained via Fourier transformation of the auto-correlation function for dimensionless pressure modulations

t independent time variable

T absolute temperature

$\mathbf{v}$ velocity vector

$\nabla\mathbf{v}$ velocity gradient tensor

$\{\nabla\mathbf{v}\}^T$ transpose of the velocity gradient tensor

v_Θ tangential-component of the local fluid velocity vector, $v_\Theta(r,z)$

$\langle z\rangle$ average depth of the cylindrical bioreactor in the z-direction (vertically downward)

Greek symbols

∇ gradient operator

β_0 stress-free Damköhler number for nutrient consumption by nth-order kinetics

β_{pressure} pressure-sensitive Damköhler number for nutrient consumption by zeroth-order kinetics

$\beta_{\text{pressure,critical}}$ critical value of the pressure-sensitive Damköhler number, above which, one must include stress-sensitive nutrient consumption in the boundary condition at the rotating cylindrical wall

γ Onsager off-diagonal coefficient that couples normal pressure stress to the rate of nutrient consumption, dimensions of inverse velocity (i.e., time/length)

γ' Onsager off-diagonal coefficient that couples dimensionless normal pressure modulations to the rate of nutrient consumption; mass per area-time

$\delta_{\text{Diffusivity}}$ nutrient/oxygen diffusivity ratio; $D_{\text{Nutrient}}/D_{\text{Oxygen}} \approx \{32/1000\}^{0.5}$

$\varepsilon_{\text{Cell}}/\varepsilon_{\text{Nutrient}}$ ratio of cell mass produced relative to nutrient mass depleted during nutrient consumption and cell proliferation

$\varepsilon_{\text{Oxygen}}/\varepsilon_{\text{Nutrient}}$ ratio of oxygen mass depleted relative to nutrient mass depleted during nutrient consumption

Θ angular displacement of the rotating cylindrical wall

Γ dimensionless ratio of fluid pressure, with and without angular velocity modulations
κ complex frequency-dependent susceptibility function
μ_i chemical potential of species i
η dimensionless spatial coordinate in the radial direction, r/R_{wall}
υ_{Heart} frequency of physiological heartbeats, ≈1 cycle/s
$\Psi_{Nutrient}$ dimensionless mass density of nutrients in the aqueous medium
$\Psi_{Nutrient,Bulk}$ dimensionless bulk mass density of nutrients in the aqueous medium
Ψ_{Oxygen} dimensionless mass density of dissolved oxygen in the aqueous medium
$\rho_{Nutrient}$ mass density of nutrients in the aqueous medium; grams/cm^3
$\rho_{Nutrient,Bulk}$ volume-averaged mass density of nutrients in the aqueous medium
ρ_{Oxygen} mass density of dissolved oxygen in the aqueous medium; grams/cm^3
σ auto-correlation function for dimensionless fluid pressure modulations
τ dimensionless time; $tD_{Nutrient}/R^2_{wall}$
$\Delta\tau$ step size in dimensionless time
$\tau_{ViscousStress}$ molecular momentum flux tensor; also, viscous stress tensor
Θ angular spatial variable in cylindrical coordinates
ω angular frequency of physiological heartbeats, $2\pi\upsilon_{Heart} \approx 2\pi$ rad/s
Ω constant angular velocity of the cylindrical wall that contains bound cells, ≈4 rpm
χ real separation constant in Eq. (15)
ξ_{A1} Onsager diagonal coefficient (i.e., αT) that couples the affinity (i.e., φ_A) to the rate of nutrient consumption
ξ_{A2} Onsager off-diagonal coefficient (i.e., γT) that couples the magnitude of the velocity gradient tensor to the rate of nutrient consumption

Acknowledgements

LA Belfiore acknowledges the Provincia Autonoma di Trento for supporting his "SmartBone" research project while on sabbatical at the University of Trento, as well as the Polymers Program in NSF's Division of Materials Research via Grant# DMR-0320980. Professor Matt Kipper in the Department of Chemical and Biological Engineering at Colorado State University provided excellent information about receptor-mediated cell-protein binding, the formation of receptor complexes, cell surface diffusion, and rates of nutrient consumption. Dr. Antonella Motta and Professor Claudio Migliaresi in the Department of Materials Engineering and Industrial Technologies at the University of Trento are acknowledged for insightful discussions about rates of cell proliferation in the presence of mechanical stress, cell-protein docking, and cell-cell attraction on protein-coated surfaces. Finally, Professor Naz Karim in the Department of Chemical Engineering at Texas Tech University provided invaluable data about cell death to justify its exclusion from this manuscript.

References

[1] K.D. Song, T.Q. Liu, Z.F. Cui, X.Q. Li, X.H. Ma, Three-dimensional fabrication of engineered bone with human bio-derived bone scaffolds in a rotating-wall vessel bioreactor, Journal of Biomedical Materials Research, Part A 86A (2) (2008) 323–332.
[2] L.A. Belfiore, M.N. Karim, C.J. Belfiore, Tubular bioreactor models that include Onsager-Curie scalar cross-phenomena to describe stress-dependent rates of cell proliferation, Biophysical Chemistry 135 (1-3) (June 2008) 41–50.
[3] D.D. Fitts, Nonequilibrium Thermodynamics—a phenomenological theory of irreversible processes in fluid systems, McGraw-Hill, 1962, pp. 34–37.
[4] S.R. de Groot, P. Mazur, Nonequilibrium Thermodynamics, New York, Dover, 1984.
[5] L.A. Belfiore, Transport Phenomena for Chemical Reactor Design, Wiley, Hoboken, New Jersey, 2003, pp. 700–702, Chapters 14, 23, 25.
[6] L.A. Belfiore, Effects of the collision integral, thermal diffusion, and the Prater number on maximum temperature in macroporous catalysts with exothermic chemical reaction in the diffusion-controlled regime, Chemical Engineering Science 62 (3) (2007) 655–665.
[7] L.A. Belfiore, Soret diffusion and nonideal Dufour conduction in macroporous catalysts with exothermic chemical reaction at large intrapellet Damköhler numbers, Canadian Journal of Chemical Engineering 85 (3) (2007) 268–279.
[8] M. Yanagisawa, N. Suzuki, N. Mitsui, Y. Koyama, K. Otsuka, N. Shimizu, Effects of compressive force on the differentiation of pluripotent mesenchymal cells, Life Sciences 81 (2007) 405–412.
[9] H. Kawashima, M. Ikegame, J. Shimomura, O. Ishibashi, T. Komori, T. Noda, H. Ozawa, Tensile stress induced osteoblast differentiation and osteogenesis in mouse calvarial suture cultures, Journal of Gravitational Physiology 7 (2) (2000) 121–122.
[10] C. Rubin, A.S. Turner, C. Mallinckrodt, C. Jerome, K. McLeod, S. Bain, Mechanical strain induced noninvasively in the high-frequency domain is anabolic to cancellous bone, but not cortical bone, Bone 30 (3) (2002) 445–452.
[11] W.T. Godbey, B.S. Stacey Hindy, M.E. Sherman, A. Atala, A novel use of centrifugal force for cell seeding into porous scaffolds, Biomaterials 25 (2004) 2799–2805.
[12] R.B. Bird, W.E. Stewart, E.N. Lightfoot, Transport Phenomena, 2nd EditionWiley, Hoboken, New Jersey, 2002.
[13] C. Reichardt, Solvents and Solvent Effects in Organic Chemistry, 2nd editionVCH, Basel, Switzerland, 1988. J.H. Espenson, Chemical Kinetics and Reaction Mechanisms, 2nd edition, McGraw-Hill Series in Advanced Chemistry, 1995 pp. 166-7.
[14] A.I. Barakat, A model for shear-stress-induced deformation of a flow sensor on the surface of vascular endothelial cells, Journal of Theoretical Biology 210 (2001) 221–236.
[15] A. Stefanovska, D.G. Luchinsky, P.V.E. McClintock, Modelling couplings among the oscillators of the cardiovascular system, Physiological Measurements 22 (2001) 551–564.
[16] A. Stefanovska, M. Bracic, Reconstructing cardiovascular dynamics, Control Engineering Practice 7 (1999) 161–172.
[17] H. Lu, L.Y. Koo, W.M. Wang, D.A. Lauffenburger, L.G. Griffith, K.F. Jensen, Microfluidic shear devices for quantitative analysis of cell adhesion, Analytical Chemistry 76 (2004) 5257–5264.
[18] J.M. Smartt, I.C. Lin, H. Ischiropoulos, R.E. Kirschner, Intermittent hydrostatic compression promotes nitric oxide production and osteo-differentiation of fetal dural cells, Annals of Plastic Surgery 55 (1) (2005) 76–80.
[19] N. Basso, J.N.M. Heersche, Characteristics of in-vitro osteoblastic cell loading models, Bone 30 (2) (2002) 347–351.
[20] V. David, A. Guignandon, A. Martin, L. Malaval, M.H. Lafage-Proust, A. Rattner, V. Mann, B. Noble, D.B. Jones, L. Vico, Ex-vivo bone formation in bovine trabecular bone cultured in a dynamic 3-d bioreactor is enhanced by compressive mechanical strain, Tissue Engineering, Part A 14 (1) (2008) 117–126.
[21] P. Yu, T.S. Lee, Y. Zeng, H.T. Low, Effect of vortex breakdown on mass transfer in cell-culture bioreactors, Modern Physics Letters B 19 (28-29) (2005) 1543–1546.
[22] H.B. Callen, T.A. Welton, Irreversibility and generalized noise, Physical Review 83 (1) (1951) 34–40.
[23] C.P. Slichter, CP, Principles of Magnetic Resonance, 2nd editionSpringer-Verlag, 1978 Chapter 2.
[24] R.B. Bird, R.C. Armstrong, O. Hassager, Dynamics of Polymeric Liquids, Volume#1, Fluid Mechanics, Wiley, New York, 1977 p. 303.
[25] J.J. Aklonis, W.J. MacKnight, Introduction to Polymer Viscoelasticity, Wiley-Interscience, New York, 1983, pp. 27–29.
[26] R.K. Pathria, Statistical Mechanics, Pergamon, Oxford, 1986, pp. 474–477.